Coastal Engineering 57 (2010) 985–995

Contents lists available at ScienceDirect

Coastal Engineering

journal homepage: www.elsevier.com/locate/coastaleng

Numerical simulation of a low-lying barrier island's morphological response to Hurricane Katrina

C.A. Lindemer [a], N.G. Plant [b], J.A. Puleo [a,*], D.M. Thompson [b], T.V. Wamsley [c]

[a] Center for Applied Coastal Research, University of Delaware, United States
[b] U.S. Geological Survey, Saint Petersburg, FL, United States
[c] U.S. Army Corps of Engineers, Vicksburg, MS, United States

ARTICLE INFO

Article history:
Received 14 July 2009
Received in revised form 21 May 2010
Accepted 8 June 2010
Available online 14 July 2010

Keywords:
XBeach
Barrier Islands
Coastal processes
Hurricanes
Chandeleur Islands
Numerical modeling

ABSTRACT

Tropical cyclones that enter or form in the Gulf of Mexico generate storm surge and large waves that impact low-lying coastlines along the Gulf Coast. The Chandeleur Islands, located 161 km east of New Orleans, Louisiana, have endured numerous hurricanes that have passed nearby. Hurricane Katrina (landfall near Waveland MS, 29 Aug 2005) caused dramatic changes to the island elevation and shape. In this paper the predictability of hurricane-induced barrier island erosion and accretion is evaluated using a coupled hydrodynamic and morphodynamic model known as XBeach. Pre- and post-storm island topography was surveyed with an airborne lidar system. Numerical simulations utilized realistic surge and wave conditions determined from larger-scale hydrodynamic models. Simulations included model sensitivity tests with varying grid size and temporal resolutions. Model-predicted bathymetry/topography and post-storm survey data both showed similar patterns of island erosion, such as increased dissection by channels. However, the model under predicted the magnitude of erosion. Potential causes for under prediction include (1) errors in the initial conditions (the initial bathymetry/topography was measured three years prior to Katrina), (2) errors in the forcing conditions (a result of our omission of storms prior to Katrina and/or errors in Katrina storm conditions), and/or (3) physical processes that were omitted from the model (e.g., inclusion of sediment variations and bio-physical processes).

Published by Elsevier B.V.

1. Introduction

Low-lying barrier islands are susceptible to extreme damage during storm events due to large waves, storm surge and run up processes. Wave run up can scour the base of dunes leading to failure, while overwash can erode dune crests creating depositional fans on the landward side of the island (Sallenger, 2000; Stockdon et al., 2006). Inundation allows wind and wave-driven currents to alter erosion and deposition patterns over the entire island surface. A relationship has been determined between the relative height of the dune and storm-induced water levels to the vulnerability of beaches during storms such as hurricanes (Sallenger, 2000; Stockdon et al., 2006). Thus, low-lying coastlines, such as Louisiana, are at extreme risk during large storm events. The most catastrophic storm events are hurricanes that have increased in frequency since 1995, perhaps due to historical multi-decadal-scale cycles (Goldenberg et al., 2001). Morphological change caused by hurricanes accounts for up to 90% of shoreline retreat in Louisiana (Kahn, 1986), where foredune heights along the coastline are normally lower than 2 m (Stone et al., 1997).

One approach to predicting vulnerability is to perform numerical simulations for barrier island evolution. Several modeling approaches exist, including those that resolve geologic details of underlying sediment, but do not resolve individual storms (Cowell et al., 1995; Rosati et al., 2006; Stolper et al., 2005), to those that resolve the coupled interactions between topography, waves, currents, and sediment transport (Cañizares and Irish, 2008; Lesser et al., 2004; Roelvink et al., 2009; McCall et al., 2010). The detailed models can resolve variations in storm characteristics, be used to evaluate restoration scenarios and aide management decisions. In order for detailed models to be useful, it is important to demonstrate the realism of simulations of specific storm events. Simulations should correspond to sensible, if not quantitatively accurate, predictions of actual storm scenarios. Previous detailed models (Roelvink et al., 2009; Jiménez et al., 2006; McCall et al., 2010; van Thiel de Vries et al., 2008) have focused on barrier islands with relatively high dunes where storm-driven overwash is an important process. We are interested in extending detailed numerical predictions to relatively low-elevation barrier islands where inundation is a dominant process.

The Chandeleur Islands (Fig. 1, showing the northern portion of the islands), are part of the Breton National Wildlife Refuge, and are

* Corresponding author. Center for Applied Coastal Research, University of Delaware, Newark, DE 19716, United States. Tel.: +1 302 831 2440.
E-mail address: jpuleo@udel.edu (J.A. Puleo).

0378-3839/$ – see front matter. Published by Elsevier B.V.
doi:10.1016/j.coastaleng.2010.06.004

located 161 km east of New Orleans, Louisiana. They form an 80 km long barrier island chain in the Gulf of Mexico and are oriented roughly north to south. The Chandeleurs are remnants of the St. Bernard Delta, formed by the Mississippi River. The islands are a significant feature in the gulf that may represent the fate of a dying barrier island; being one of the most rapidly receding island systems in the United States (Kahn, 1986). The topography in some areas is extremely low, with elevations in our focus region that were uniformly less than 2 m.

During the hurricane season of 2005, the islands were impacted by several hurricanes, most notably Hurricane Katrina. This hurricane is one of the costliest storms, in both fatalities and damage, to ever make landfall in the United States. It struck the Atlantic coast of Florida as Category 1 on the Saffir–Simpson Scale. It then crossed the Florida peninsula into the Gulf of Mexico and rapidly strengthened to Category 5, before making landfall as a Category 3 west of the Chandeleur Islands (Knabb et al., 2005). The high storm surge and strong waves resulted in island fragmentation with numerous breaches that exposed wetland once protected by beaches and dunes. Based on comparisons of lidar surveys, approximately 82% of the island area was lost between 2002, just after Hurricane Lili, and 2005, just after Hurricane Katrina (Sallenger et al., 2009).

Fig. 2 shows satellite imagery of the evolution of the islands from 2001 to 2005, and the development of the islands from a continuous chain to a highly disconnected group. The islands during this time period were battered by hurricanes Lili (03 Oct 2002), Isidore (26 Sept 2002), Ivan (16 Sept 2004), Cindy (05 Jul 2005) and Katrina (29 Aug 2005). The storm tracks of these hurricanes are highlighted in Fig. 1. It is obvious that in several locations the islands completely disappeared (north section of islands) and sediment was washed away throughout the chain, leaving only marshland (Fig. 2).

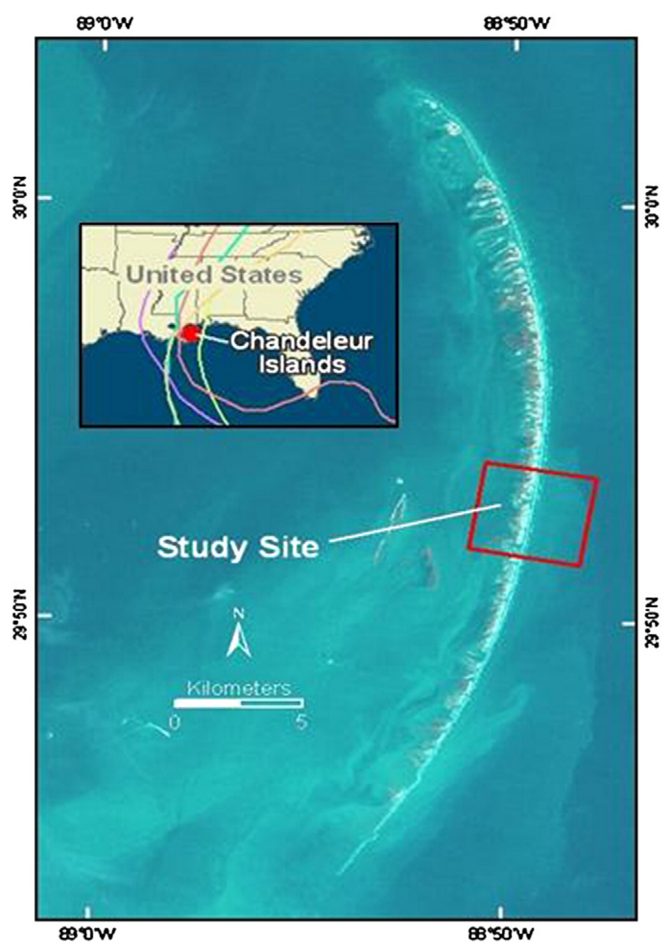

Fig. 1. Chandeleur Islands, study site highlighted in red box. Recent hurricane tracks are shown in the inset, with: purple — Lili (2002); aqua — Isadore (2002); green — Ivan (2004); beige — Cindy (2005); Pink—Katrina (2005). (Landsat satellite imagery, 2004).

A recently introduced numerical model, XBeach (eXtreme Beach behavior model), implements morphological modeling of dune erosion, overwash, inundation, and breaching (Roelvink et al., 2009). Roelvink et al. (2009) demonstrate that the model skillfully simulates storm hydrodynamics including short- and long-wave heights and associated currents as well as predicting sediment transport associated with dune erosion. In particular, they demonstrate that the model can recover observed variations in dune erosion associated with storms that struck Assateague Island on the U.S. east coast. The variations in erosion response depended on variations in the initial topography, that ranged from relatively high dunes (>4 m) to relatively low dunes (<2 m). These storm conditions were spatially homogeneous, with storm surge elevations close to 1 m and offshore wave heights of about 4 m such that dune overwash occurred where the dune height was less than about 2 m. This study indicated that variations in the storm conditions (i.e., surge height, wave height, and wave period) could also control the degree of dune erosion, primarily by increasing or decreasing the intensity of dune overwash.

In the case of low-lying islands, such as the Chandeleur Islands, inundation (i.e., submergence) occurs during major storms and this process can substantially alter island topography and planform areas (Fig. 2). Processes that are resolved by the XBeach model should be able to account for this island erosion scenario. We use XBeach to make detailed predictions of the response of a portion of the Chandeleur Islands to the sediment transport processes driven by Hurricane Katrina. Surge elevations at the island were predicted to be nearly 4 m and wave heights exceeded 5 m offshore (IPET, 2007). The following section describes the numerical model and the data sets that were used to initialize, force, and evaluate the model (Section 2). The model simulation results are presented (Section 3). Section 4 includes discussions of how subtle changes in the spatial (Section 4.1) and temporal resolution (Section 4.2) of the model impact the simulation results. We explore the impact of the omission of storms that occurred between the initial island survey in 2002 and Hurricane Katrina in 2005 (Section 4.3) and discuss the omission of geologic variation in sediment properties (Section 4.4). Conclusions are given in Section 5.

2. XBeach model

XBeach is a coupled hydrodynamic and morphodynamic model that can be used to test a range of morphological modeling concepts and resolve processes at relatively small spatial, O(1 m), and temporal, O(1 s), scales. It is capable of handling extreme conditions, including hurricanes. Processes that are resolved by the model include wave-averaged evolution of short waves, time-resolved evolution of long waves, wave-driven flows, sediment transport, and morphological change. For an in-depth description of XBeach, see Roelvink et al. (2009). For the purposes of this study, we require a morphological prediction that depends on hurricane-driven processes. Morphologic change is obtained from XBeach from the sediment mass conservation equation, wave- and flow-driven sediment transport parameterizations, wave energy conservation, and momentum conservation.

A key formulation in the morphological evolution problem includes a formal separation of the fast time scales associated with hydrodynamic processes and the relatively slow evolution of the

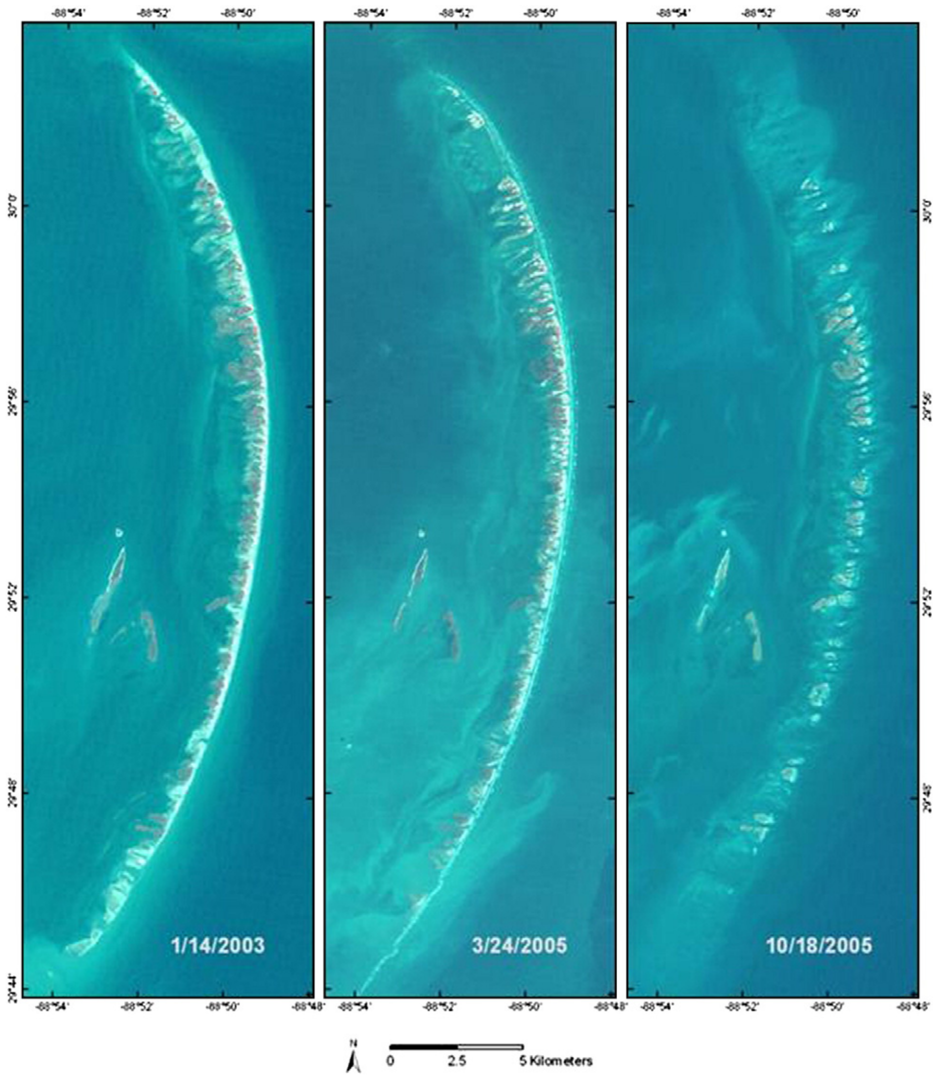

Fig. 2. Recent hurricane effects on the Chandeleur Islands. (Landsat satellite imagery).

morphological features of interest. This separation makes it possible to decrease computational time. This is done by using a time scale multiplier, or morfac, to sample the hydrodynamic inputs and to apply a multiplier to the morphologic response. This is implemented as

$$\frac{\partial z}{\partial t} = -\frac{m}{(1-p)}\left(\frac{\partial q_x}{\partial x} + \frac{\partial q_y}{\partial y}\right), \quad (1)$$

where z is the spatially and temporally varying bed elevation, q_x and q_y are the corresponding sediment transport rates, p is the sediment porosity (0.4 for this simulation), and m is the adjustable morfac parameter that separates morphological and hydrodynamic time scales, in order to speed up morphological response. The implementation allows the hydrodynamics to be computed on a fast time scale, Δt, but the morphology and boundary conditions change slowly, with a time step of $\Delta\tau$, where $\Delta\tau = m\ \Delta t$. To implement this consistently, the boundary conditions (i.e., wave parameters and water levels) are updated using the large time step as well. So, for example, at the nth computational time step, the fast hydrodynamics are computed and stored at t_n ($=n\Delta t$) while the bed level is computed and stored at τ_n ($=nm\Delta t$). Boundary conditions, B_n ($=B[\tau_n]$), are sampled from the input time-series with this larger time step, $\Delta\tau$. If, for $m>1$, bed level and boundary condition changes are indeed small at the short time scale, then this approach should yield an accurate approximation of the short-scale averaged morphological response. Implications of this approach include sub-sampling the boundary conditions and altering the coupled model feedback mechanisms. Lesser et al. (2004) discuss these effects in an application to another numerical model. The sole benefit of the approach is to reduce computation time for a problem that spans a broad range of time scales. For example, a simulation that takes 50 h to run with $m=1$, would take 5 h using $m=10$.

The sediment transport formulations are described by Roelvink et al. (2009) and McCall et al. (2010). A depth-averaged advection–diffusion scheme with source and sink terms is used to model sediment concentration in the water column, varying on the long-wave time scale. The sediment transport formulations are applied to a single sediment type that is defined by grain-size and density parameters. As is true with most study sites, the Chandeleur Islands contain numerous sediment types, including marsh, mud, peat and sands, each with unique transport rates. We will address this model-implementation limitation in the discussion.

The flow model is based on the nonlinear shallow water equations at a time scale that resolves long waves forced by wave groups but not individual short waves. Wave-averaged equations are used to determine the short wave energy conservation given offshore boundary conditions that resolve wave directional distributions while assuming a narrow-banded frequency spectrum. Wave energy dissipation is fed to a roller model, and roller dissipation contributes to radiation stress gradients that force slowly-varying currents.

2.1. Model domain

The model domain used is a 4 km × 4.5 km section of the islands (Fig. 1). The domain uses a grid resolution of 20 m in the alongshore direction and a spatially varying cross-shore grid resolution that ranges from 20 m offshore to 10 m in the area of interest around the islands. Discussion of the choice for resolution is given in Section 4. The boundary conditions applied to the model include wave height, direction, and peak period on the gulf-facing offshore boundary. Additionally, four storm surge elevation time-series were applied at each corner of the domain and interpolated alongshore to constrain the seaward and landward boundaries for the duration of the simulation. The hydrodynamic conditions used are discussed in Section 2.2. The initial bed elevation was obtained from a smooth interpolation of the pre-storm lidar data and offshore bathymetry (Section 4.3).

2.2. Hydrodynamic conditions

Forcing conditions were provided by the United States Army Corps of Engineers (USACE). Data include wave, water level, and flow inputs (Fig. 3). Significant wave heights were simulated using the STWAVE model (Smith et al., 2001) driven by the hurricane wind field. The spatial resolution used in STWAVE was 200 m. STWAVE was forced at the offshore boundary by the WAM model with 30 s temporal resolution. STWAVE was coupled to ADCIRC (Luettich et al., 1992) at 30-minute intervals. STWAVE received updated water levels from ADCIRC using the same wind fields that were used in ADCIRC. ADCIRC received updated wave radiation stress gradients from STWAVE in

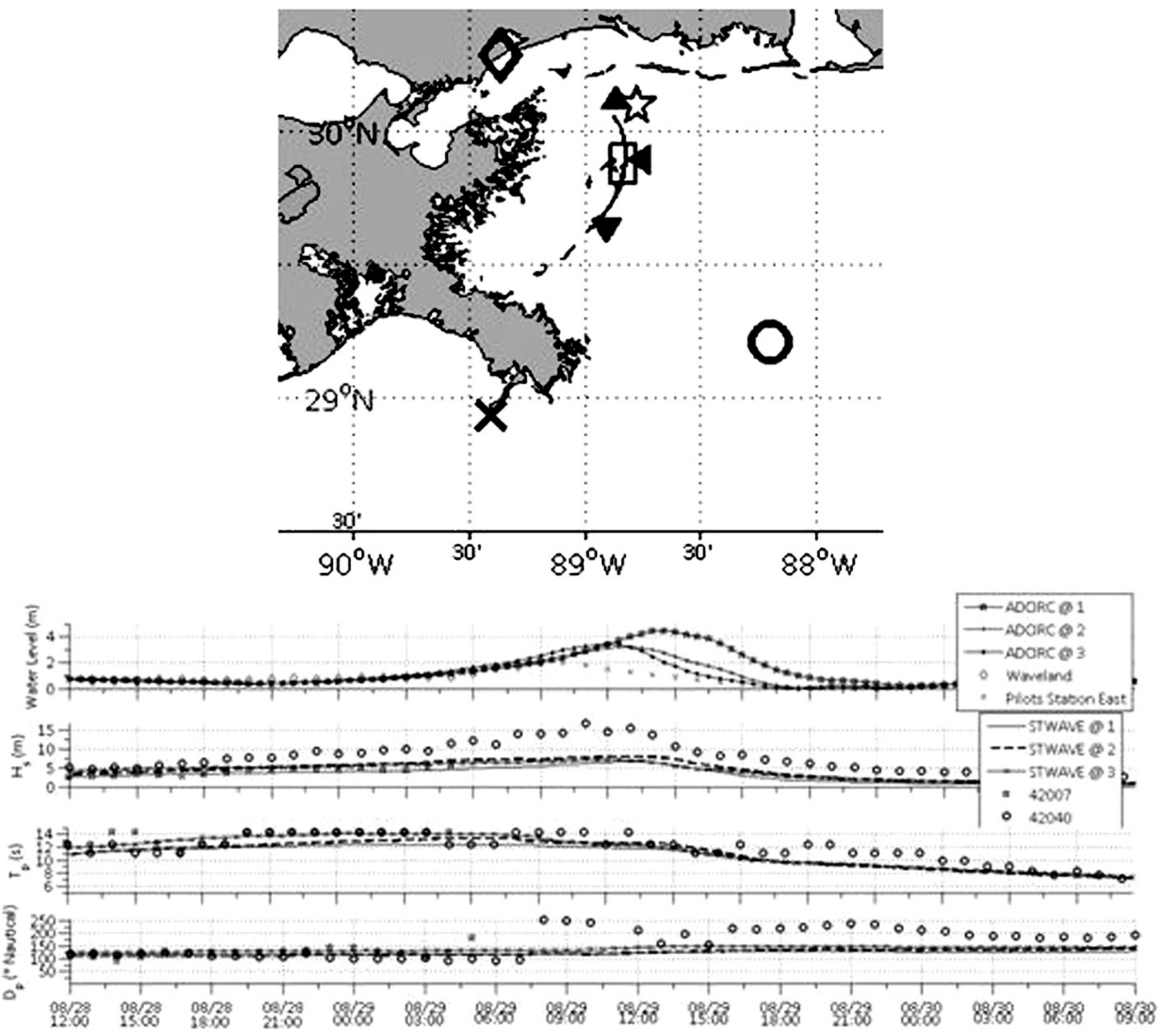

Fig. 3. Location of forcing condition inputs (top panel). The study site is boxed. Locations are: ADCIRC/STWAVE 1 ▲, ADCIRC/STWAVE2 ▼, and ADCIRC/STWAVE3 ◀. Tide gage data locations are: Waveland □, and Pilots Station East x. NOAA wave gage data was collected at two locations denoted by a star (gage 42,007) and an open circle (42,040) Forcing conditions used for the study site during Hurricane Katrina (lower panels). The forcing variables from top to bottom are are water level, significant wave height (H_s), peak wave period (T_p), and mean wave direction (D_p).

order to compute wave setup (IPET, 2007). These models have been used for post-storm analysis by the USACE in comparing the outputs from the STWAVE and ADCIRC data set to observational data collected during Hurricane Katrina (IPET, 2007). Prediction errors for STWAVE ranged from 0.1 to 0.3 m under prediction of wave height during the storm peak in the inland waters of Lake Pontchartrain. Errors were less than 1 m in the domain just offshore of the Chandeleur Islands. Extensive comparisons can be found in the IPET report. ADCIRC predicted storm surge was strongly correlated with observed high watermarks ($R^2 = 0.82$) and, on average, under predicted the elevations by 0.18 m (IPET, 2007).

Model data from STWAVE, ADCIRC and observational data obtained from NOAA gages 42,007 (near the north end of the Chandeleur Islands), (Fig. 3) and 42,040 (offshore) and two tide gages (Waveland, MS and Mississippi Pilot Station East) are consistent. Modeled values were extracted from three different locations (named ADCIRC/STWAVE 1, 2, 3) that were relatively close to the observation locations (Fig. 3). The predicted storm surge at all locations was similar to the observations before the storm peak, prior to failure of the Waveland gage. The predicted surges at the Chandeleur Island locations far exceeded the measurements, but this is consistent with the previous analyses of the actual spatial patterns of observed storm response (IPET, 2007). Wave height, period, and direction at ADCIRC/STWAVE 1 compared well with observations from gage 42,007, (Fig. 3). The gage failed before the storm reached its peak, so we include comparisons to the offshore gage. Predicted wave heights were different, as expected, while wave periods compare well with those from the offshore gage throughout the duration of the simulation. At the offshore location, wave directions near the peak of the storm approach from a southwesterly direction, differing from the model predictions near the Chandeleurs. This is likely due to the differences in the geographic settings, since the Chandeleurs do not receive ocean waves from the west.

Hydrodynamic predictions from ADCIRC at the locations matching the onshore and offshore boundaries of the XBeach domain were used as XBeach water level boundary conditions. Flow velocities were not used in the simulation. The wave information from STWAVE was used to produce a parameterized Jonswap spectrum of the short wave information to XBeach. These data were applied only to the offshore boundary, with no waves being forced from the back bay (west) region. The model was forced from 28 Aug 2005 00:00 to 30 Aug 2005 12:30. Storm surge elevation reached a peak value of 3.5 m. The peak significant wave height was 5.7 m with a mean wave period of 12.7 s (Fig. 3). The mean wave direction was initially 110 nautical degrees as the storm approached the islands, rotating to 135 nautical degrees as the storm left the Chandeleurs.

2.3. Bathymetry

Bathymetry data used to initialize the bed level was produced using a fusion of airborne lidar topography and ship-based sonar bathymetry. The most recent lidar survey prior to Hurricane Katrina was completed on 18 Oct 2002 after Hurricane Lili struck the island and was collected using NASA's Airborne Topographic Mapper, ATM, (Brock et al., 2002). There were several hurricanes that affected the region in the time between the initial lidar survey and Hurricane Katrina. Although this results in a discrepancy between true pre-Katrina topography and the initial topography input to the model, it is the best available data. The bathymetry input for the study site required inclusion of offshore bathymetry data that was sampled in 2006 and 2007 (Twichell et al., 2009). These data post-date Katrina's landfall, but our assumption is that discrepancies in the offshore region will have minimal impact on the waves and water level prediction over the island itself. This assumption is supported by Roelvink et al. (2009) who showed that morphologic response was not sensitive to substantial variations in the submerged foreshore slope. Lidar and bathymetry data were assimilated using spatial interpolation that included smoothing and also enforcement of minimum gradients on lateral boundaries (Plant, et al., 2002; Plant et al., 2009). The initial interpolation included both the lidar and bathymetry data, interpolating them to a coarse resolution (100 m cross-shore and 500 m alongshore) domain. The data were weighted according to assumed uncertainties:

$$\sigma_{bathy} = \varepsilon_{bathy} \exp\left(\left[\frac{z_{bathy} - z_0}{d_{bathy}}\right]^2\right), \tag{2}$$

$$\sigma_{lidar} = \delta_{lidar} + \varepsilon_{lidar} \exp\left(\left[\frac{z_{lidar} - z_0}{d_{lidar}}\right]^2\right) \tag{3}$$

where ε_{bathy} (10 m) are possible elevation errors due to changes in the island topography, z_0 (0.0 m) are elevations where these errors are maximum, d_{bathy} (2 m) is a decay scale to control where the errors become negligible (i.e., at depths of about three times d_{bathy}, the bathymetry data are assumed to be error free). Likewise, lidar errors result from expected system errors ($\delta_{lidar} = 0.15$ m) and error associated with lack of penetration of the laser to the bottom ($\varepsilon_{lidar} = 10$ m and $d_{lidar} = 1$ m). These formulations generally allow bathymetry to dominate the interpolation in deep water (depths greater than 1–2 m), and allow the lidar to dominate the topography. A second iteration of the interpolation scheme created a high resolution bathymetry (10 m cross-shore and 20 m alongshore) using the lidar data alone and updating the low resolution "prior" estimate. The high resolution result was identical to the low resolution where there was no lidar data. It reflected the detail of the lidar data at higher elevations and transitioned smoothly into the bathymetric data.

Post-storm lidar data were collected on 01 Sept. 2005. Because these data were not used as model input, it was not necessary to assimilate the bathymetry data. Instead, spatial interpolation was used to filter spurious measurements. Unreliable interpolation estimates were rejected if sample errors describing ability to reduce noise, exceeded 25% (Plant et al., 2002), or root mean-square (RMS) errors (describing lidar clutter) exceeded 0.5 m. Ambiguity associated with distinguishing low-lying topography from the sea surface required using additional information from color-infrared satellite imagery to classify land and water. The classification was trained over manually selected patches of land and water that determined the correlation of three color channels (red, green, and blue) to either land or water. The classification was imperfect and returned information on its uncertainty so it was, in turn, assimilated with the interpolation elevations as follows. Data were rejected if the imagery strongly contradicted the topographic data. That is, data were rejected if the image classification was confident that the scene included water but the elevations exceeded −0.5 m. Likewise, data were rejected if the classification was confident that the scene included land, but the elevation was below −0.5 m. The post-storm topography that survived the assimilation with the imagery (Fig. 4) was used to assess the model simulation's predictive skill.

3. Results

The conditions chosen to represent Hurricane Katrina caused inundation for a majority of the simulation period at the study site. Maximum water levels over the island were almost 4 m above mean sea level. Given that initial island heights in the study region were at most 2 m, the island would have been inundated even if it had not suffered from erosion. Based on the observational data, it is apparent that the island was breached in numerous locations and that the island elevations were greatly reduced in the regions that did not breach (Fig. 4). Within the XBeach model domain, the observations

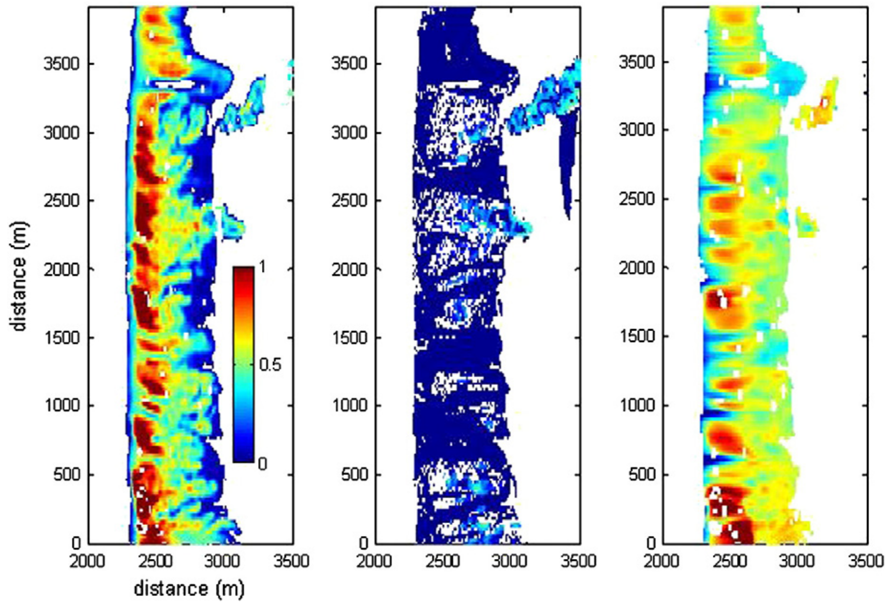

Fig. 4. Topography from the initial survey (left), post-Katrina survey (middle), and post-Katrina simulation (right). Data were masked (blank areas) where there was poor lidar coverage or sample root mean square variance exceeded 0.5 m or lidar elevations were inconsistent with image interpretation. Post-Katrina topography that converted to open water (based on image analysis) is shown as "deeper" regions—the actual depth in these areas is unknown.

indicate that 90% of the island area with elevations above mean sea level was lost between 2002 and 2005; all of the area with elevation exceeding 0.5 m was lost; and 80% of the area with elevation above −0.5 m was lost (based on comparing lidar surveys between these time periods).

The simulated post-Katrina topography is shown in Fig. 4. The data mask used to filter the initial topography was used to filter the simulated topography so that visual comparisons can be made where the original data were accurate. The simulated morphodynamics eroded higher topographic features and tended to smear them in the cross-shore direction and increased the amount of island dissection. While the simulated elevation-lowering and dissection is qualitatively consistent with the observations, the simulation did not produce the same degree of dissection and island lowering that is apparent in the post-storm observations. Many of the areas that appear as only nearly-breached in the XBeach results correspond to regions that were actually converted to open water (shaded blue in the post-storm survey map). The mean simulated elevation change over the island was about 0.06 m (erosion), and the maximum simulated erosion was about 1 m where incisions cut through the highest topography.

We investigate in more detail the correlation between observed and simulated changes. In Fig. 5, the observed change, (the difference between lidar-surveyed initial and final topography) is plotted against simulated change (the difference between XBeach initial and final topography). A perfect correspondence between observation and simulation is indicated by the dashed line. Points below and parallel to this line show that the simulated erosion is correlated to the observations. An offset relationship is apparent, where the post-storm elevation is under predicted by 0.5–1.0 m. The under prediction may be explained by the fact that the initial topographic data significantly pre-dates (by three years) Katrina's landfall as it is apparent that there was substantial pre-Katrina evolution (Fig. 2). This possibility will be addressed in Section 4.3.

More information for this analysis was extracted by utilizing the image-based classification of land and water associated with the post-storm topography (no bathymetry was available for comparison). Points marked with black in Fig. 5 represent locations where the observed topographic elevations from lidar were above the mean water level both before and after Katrina. Gray points represent locations where elevations were observed to be above mean water

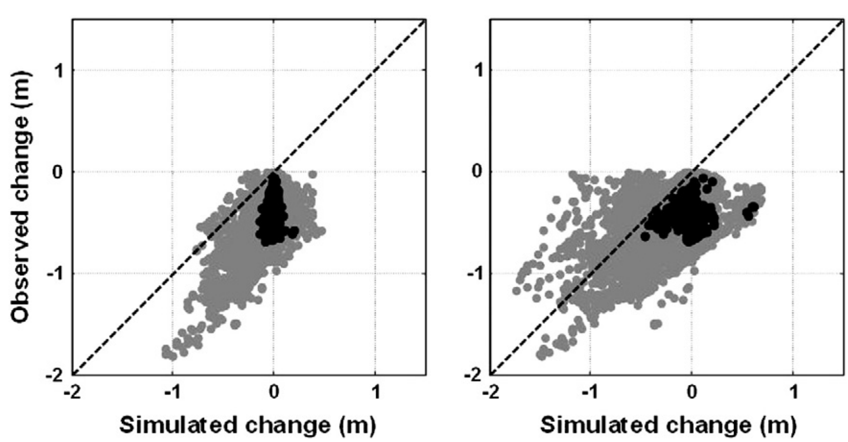

Fig. 5. Comparison of observed and predicted changes. The changes are shown for simulation of a single Katrina storm (left) and simulation of four consecutive storms (right). The black symbols represent locations where observed topographic elevations were above the mean water level both before and after Hurricane Katrina. The gray symbols represent locations where observations indicate that topography was converted to bathymetry.

level prior to Katrina and were below mean water after the storm—i.e., they were converted to open water. To make this comparison, the post-storm elevations of regions that were under water were assumed to be at least at the mean water level. We created an augmented elevation model with the missing data replaced with 0.0 m elevation. Thus, if a grid elevation from the pre-storm survey was 2.0 m and the final elevation was missing, but clearly submerged, then an augmented "observation" based on the imagery would indicate 0.0 m elevation. The "observed" elevation change would be estimated as −2.0 m and would likely be an underestimate of the true change. However, it allows us to determine if the model can accurately predict the locations of severe erosion. This classification of the results indicates that the simulated changes were correlated to the observations ($R^2 = 0.42$) when there were large enough changes to convert topography to open water. Topography that survived on the landward side of the island was observed to erode. However, the simulations predicted little or no elevation change and these predictions were not correlated to the observations ($R^2 = 0.02$). Further discussion of the statistical analysis can be found in Section 4.3.

Fig. 6 describes in more detail the differences between the observed and modeled changes. Observed erosion includes removal of grass-covered berm (labeled *brm*) at the back of the beach (*bch*) and island lowering across the entire barrier platform. Vertical exaggeration makes the beach appear as a steep slope. Its actual slope is about 1:50. The model predicted the berm erosion as well as some profile migrations that were below the mean water level (and thus, not observable in the post-storm lidar survey). Landward of $x = 2800$ m, prominent features are recognizable in both pre-storm and post-storm photographs, in the lidar map, and in the elevation cross-section. This suggests that there was little erosion or deposition at the landward side of the island. Specifically, there was no evidence of overwash deposits in either the observations or model simulation. Island response in this scenario is different from the results of previous studies that focused on overwash-driven sediment transport. Fig. 7 shows the elevation changes over the full study area that were both observed and simulated. Observations suggest that erosion occurred over the entire island surface—there was no deposition. In the simulation, maximum erosion occurred along the berm crests, and deposition occurred both in front of and behind the original berm locations. The largest amount of deposition corresponded to infilling of local depressions. There is no evidence of an overwash fan.

4. Discussion

There are a number of inherent errors with hindcast simulations using numerical models. In modeling with XBeach, we are interested in understanding the possible sources of error to explain the under prediction of simulation results compared to the erosion inferred from the lidar data. For instance, the boundary forcing, with simulated hydrodynamic conditions, may have produced conditions that were not an accurate representation of Katrina's forcing. However, this is not a likely error source since (1) the boundary forcing conditions have been extensively evaluated and errors in surge and wave height are relatively small compared to the maximum values and (2) the evidence for inundation regardless of these errors is overwhelming. A sensitivity study was completed evaluating how small changes in the forcing conditions would affect the final morphology. It was found that small changes in the forcing conditions resulted in only small changes in the model skill, highlighting that small errors in the hydraulic boundary conditions did not result in excessive errors in the simulated bed elevation.

Alternatively, the physical processes that were resolved with the model equations may not have captured all of the dominant processes. For instance, the presence of vegetation is ignored in our implementation. It is possible that the important processes were not adequately resolved by the spatial or temporal resolution of the model. The temporal resolution is of interest because of the implementation of the separation of morphological and hydrodynamic time scales. We examine the influence of variations in the morfac parameter, *m*. Furthermore, the initial topography (sampled in 2002) cannot be accurate as an appropriate initial condition for a storm occurring three years later. We investigate the impact of changing the spatial grid resolution of the initial topography, thereby "smearing" the topographic details in order to determine if grid resolution errors are relevant. Finally, we examine the impact of including additional storms on the simulation accuracy.

4.1. Spatial resolution sensitivity study

The spatial resolution used in the analysis presented so far was 10 m cross-shore and 20 m alongshore and was chosen to minimize errors that might result from under-resolving short-scale topographic features such as the berm and other features shown in the island cross-section (Fig. 6). The overall domain size included 66,300 computational nodes. Because the choice of resolution might affect the results, two additional grid resolution scenarios were tested. A grid with a finer resolution than the original grid was chosen with a

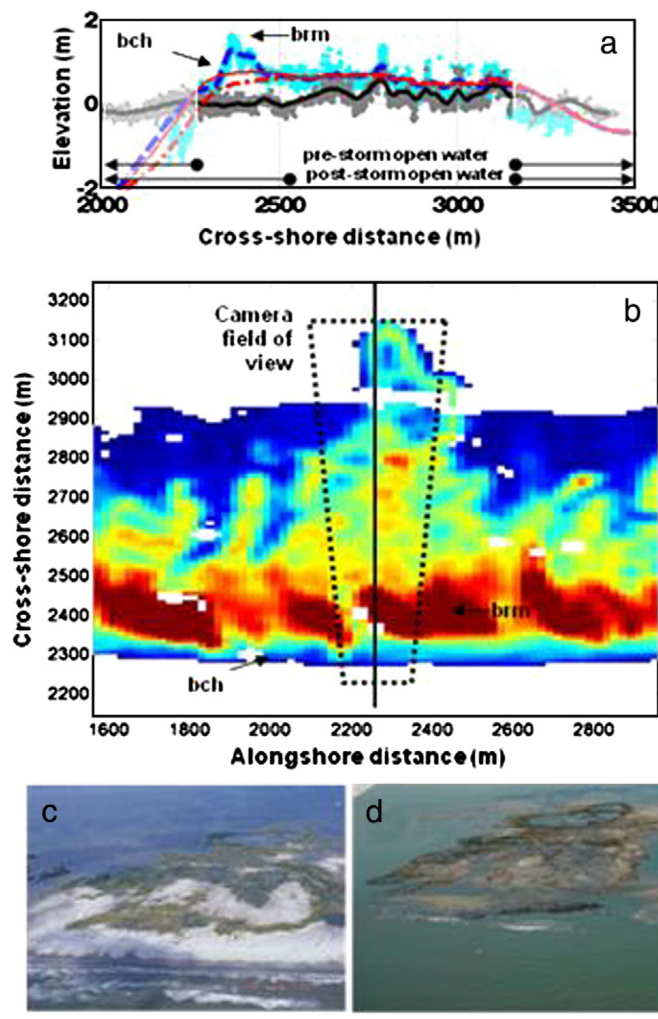

Fig. 6. Observed (a) pre-storm (blue line; dots show raw data) and post-storm (black) lidar and post-storm model elevation cross-sections (red; solid line = one storm simulation; dash–dot = 3 storm simulations). Open water areas have been masked with light transparency. The map view (b) shows the cross-section location and the viewpoint corresponding to pre- and post-storm photographs (c,d).

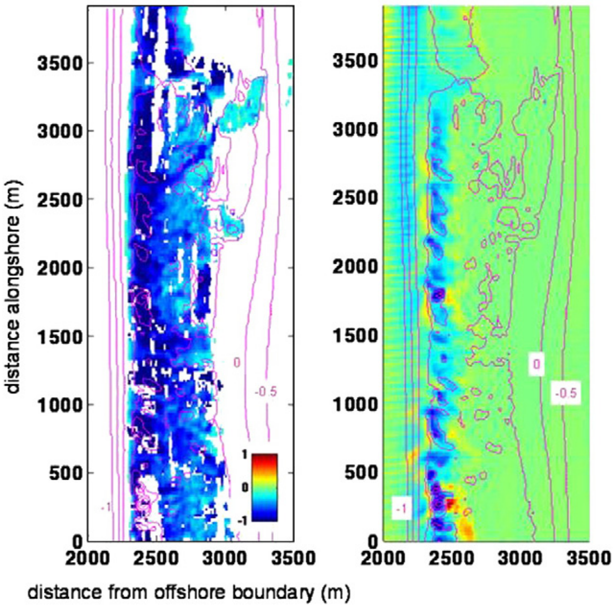

Fig. 7. Color maps showing observed (left) and simulated (right) island elevation changes (meters). Deposition is shown as warm colors and erosion as cold colors. Contours show initial island elevations (interval 0.5 m).

domain that had 188,370 computational nodes, an alongshore grid spacing of 10 m and a cross-shore resolution of 5 m in the area of interest. A coarser resolution was selected that had an alongshore grid spacing of 40 m, and a cross-shore spacing varying from 50 m offshore to 30 m in the areas where significant topographic changes were observed and required 11,368 computational nodes. The rms difference between the finer resolution (taken to be more faithful to the real topography) and the original grid was 0.06 m, which is less than the expected lidar system errors. The difference between the coarse and fine resolution was also about 0.06 m. This indicates that all three spatial resolutions were generally adequate for resolving the initial topography.

The finer and coarser resolutions were used to simulate the response to Hurricane Katrina. The variations in resolution altered the level of detail of the simulated morphological evolution (Fig. 8). The coarse resolution simulation lacks fine-scale details of the smaller cuts and berm features while the output from the fine resolution simulation captures small-scale morphological features. However, given that there were substantial uncertainties in the model inputs, it is not clear that the higher resolution is justified. In order to quantify these results, the relative error in the island elevation predictions, *RE*, is calculated as

$$RE = \frac{(XBeach_{Final} - lidar_{Final})}{(|lidar_{Final} - lidar_{Initial}| + \sigma_{lidalError})}, \quad (4)$$

where the relative error is the difference between the XBeach final data, $XBeach_{Final}$ and lidar post-storm data, $lidar_{Final}$, compared to the magnitude of change in elevation between lidar post-storm, and lidar pre-storm, $lidar_{Inital}$, plus an additional error term. The additional error term, $\sigma_{lidar\ Error}$, is related to GPS error associated with lidar data (~0.2 m), and temporal errors (~0.25–1.0 m). Assuming that the temporal error is 0.4 m, $\sigma_{lidar\ Error}$ is found to be 0.45 m when calculated with

$$\sigma_{lidar\,Error} = \sqrt{(GPS\ error\ )^2 + \ (Temporal\ error)^2}. \quad (5)$$

The *RE* was calculated for the three resolution cases (Table 1).

Relative errors greater than 1 signify serious failure of the model, as the magnitude of the errors would exceed the magnitude of changes that we intended to predict. The three resolutions tested in this study all showed *RE* less than 1, indicating the model did not fail in any of the three cases. However, the *RE* was typically greater than 50%. The errors were also similar, varying 1% at maximum, for each of the resolutions, indicating that the highest resolution implementation, which was the most computationally expensive, did not provide significant benefit over the medium and coarse resolutions. It is clear from this analysis that the coarse resolution would actually suffice for simulating this scenario in spite of the apparent loss of detail. The apparent lack of preference for high resolution may be due to the fact that the post-storm topography was devoid of major short-scale features. Compared, for instance, to remnant high dunes in the McCall

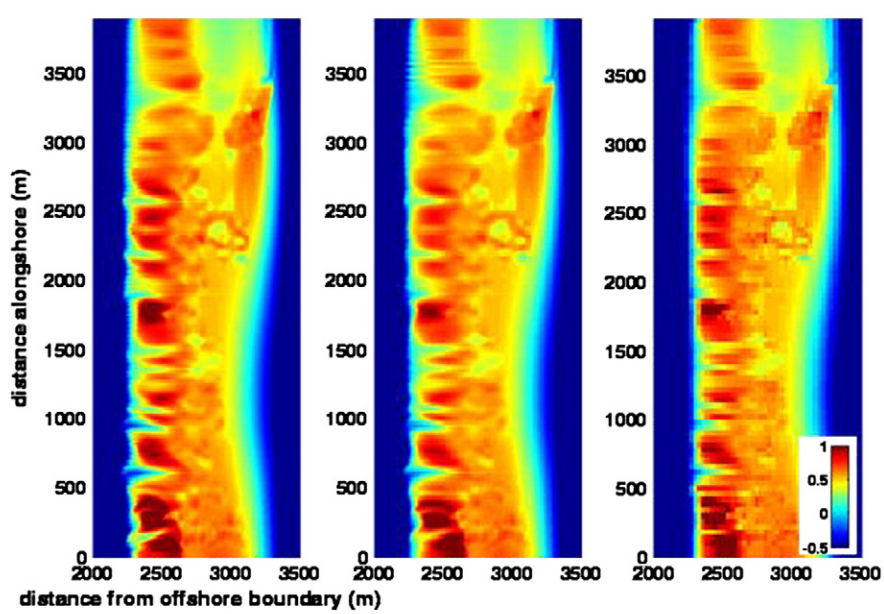

Fig. 8. Simulation results using fine (left), medium (middle), and coarse (right) grid resolutions. Color scale is elevation in meters.

Table 1
Relative error as a function of grid resolution.

Relative error bins for resolution			
Relative Error	Fine	Medium	Coarse
R.E.>100%	0.000	0.000	0.000
100%>=R.E.>75%	0.106	0.098	0.097
75%>=R.E.>0%	0.718	0.719	0.728
50%>=R.E.>25%	0.110	0.118	0.111
25%>=R.E.>10%	0.016	0.014	0.015
10%>R.E.	0.011	0.011	0.011

et al. (2010) study of Santa Rosa Island, the Chandeleurs are well-resolved with the coarse resolution.

4.2. Temporal resolution sensitivity study

The sensitivity to the morfac parameter, *m*, was also tested. As with the spatial resolution, we used both finer (value of 1) and coarser (value of 20) parameterizations compared to the original choice of 10. Again, the relative errors associated with each simulation were calculated (Table 2), and indicated there was little to no difference, 2% at most, in errors under different morfac values. Again, it is clear that coarser temporal resolution of the morphologic response would have been justified and that little would be gained from finer resolution. This may be related to the magnitude of the initial condition errors, which, perhaps, dominate other error terms and reduce sensitivity to choices in factors such as morfac parameter or grid resolution.

4.3. Multiple runs

To explore the impact of using out-of-date initial topography, it is of interest to see how the Chandeleur Islands evolve after several severe hurricanes impact the island. Ideally, we would simulate all of the actual storms occurring since the 2002 lidar data were collected. However, this would be computationally prohibitive and is beyond the scope of this study. Instead, we simulated the effect of multiple storms by running several Katrina-type events over the island to determine how XBeach predicts this morphologic evolution over multiple events. Since there were several storms between the survey conducted in 2002 that provided initial bathymetry data and landfall of Hurricane Katrina in 2005, it is possible that simulation of intervening storms could reduce the mismatch between the observed and simulated post-Katrina topography. Instead of simulating the intervening storms (Lili, Isidore, Ivan, and Cindy), we use sequential forcing based on Katrina as a proxy.

Three additional storm simulations were conducted using the original choices of grid resolution and morfac, *m*. The topography after the first through fourth simulations is shown in Fig. 9. Breakup of the islands becomes more pronounced as cuts grow and deepen. After each consecutive run of Hurricane Katrina storm conditions, additional losses of subaerial island area and generally lower elevations result. On average, 2% of the initial (2002) island area was lost after each run, and a total of 8.4% is lost between run one and four. By the fourth run of Katrina, morphology starts to resemble the post-Katrina structure of the islands, with heavy segmentation. The statistical analysis of the results was based on two classes of points that were divided according to whether land was converted to open water or not. In this case, land was defined as topography with elevation above −0.5 m (Fig. 5, right-hand panel). (A discussion of datum choice is given in Section 4.2.) Locations where observations showed that the initial topography was not converted to open water (i.e., land-to-land points) were not correlated to the simulated changes given one Katrina run, as mentioned before (Fig. 5). Table 3 indicates the change in the simulation errors as a function of the number of simulated storms. Land-to-land points after multiple runs showed slight reductions in the mean error as the subsequent storms increased the total amount of erosion. Other statistics that were computed included the total root mean square error (which include both mean and random errors), and the skill (squared correlation of the regression). For the land-to-land points, the skill and the total error are not affected. XBeach has no skill predicting the variation in erosion of these points, most likely due to the points being marshland but modeled as sand in XBeach (see Section 4.3).

Points that were observed to develop from land to open water (land-to-water) showed a strong correlation between simulated and observed changes over a single Katrina run. Specifically, these points yield a regression gain of about one, and a regression skill of 0.4 (Table 3). With additional runs of Katrina, the mean error was reduced as elevations generally become lower. The total error (includes both mean and random components) decreases until three simulations have been performed. The gain and skill degrade under further simulations. This reflects the increased scatter in the correlations shown in Fig. 5. The total error is nearly constant after three simulations, suggesting that a balance is reached between improved simulation accuracy as island height is reduced and reduced accuracy due to poorly-predicted details as the island is dissected. This is further suggested by Fig. 9, where the simulated island development begins to resemble better the appearance of the islands post-Katrina. However, the exact location of cuts and remnant berms are poorly-predicted, adding to increased total errors.

4.4. Limitations due to simplified sediment characteristics

As with many coupled modeling systems that include sediment transport, XBeach uses one sediment type, sand in this case. A single sediment type does not describe accurately the sediment characteristics of the islands (see Figs. 1 and 2), that include marsh, mud, peat and sands. In modeling the development of barrier islands, sediment variability has been shown to be important (Rosati, et al., 2006). Sediment type varies spatially and vertically and the location of the layers and depths associated with each sediment type are unknown and do not exist for pre- and post-storm events. However, it is generally known that the gulf side of the islands is covered with a veneer of sand, while the Back Bay areas are characterized by a vegetated marsh with clay and mud (e.g, Twichell et al., 2009). In principle, we might expect that the sandy gulf side of the island,

Table 2
Relative error as a function of morphological acceleration.

Relative error bins for morfac			
Relative error	Morfac 1	Morfac 10	Morfac 20
R.E.>100%	0.000	0.000	0.000
100%>=R.E.>75%	0.098	0.098	0.106
75%>=R.E.>50%	0.725	0.719	0.705
50%>=R.E.>25%	0.109	0.118	0.126
25%>=R.E.>10%	0.017	0.014	0.015
10%>R.E.	0.012	0.011	0.010

Table 3
Error and skill parameter for multiple Katrina simulations.

	Mean error (m) land (water)	RMS error (m) land (water)	Skill (m) land (water)
Persistence	0.38 (0.48)	0.40 (0.55)	–
1 Katrina	0.37 (0.41)	0.39 (0.46)	0.01 (0.41)
2 Katrinas	0.36 (0.36)	0.39 (0.43)	0.00 (0.35)
3 Katrinas	0.35 (0.30)	0.39 (0.40)	0.00 (0.34)
4 Katrinas	0.35 (0.24)	0.39 (0.41)	0.00 (0.31)

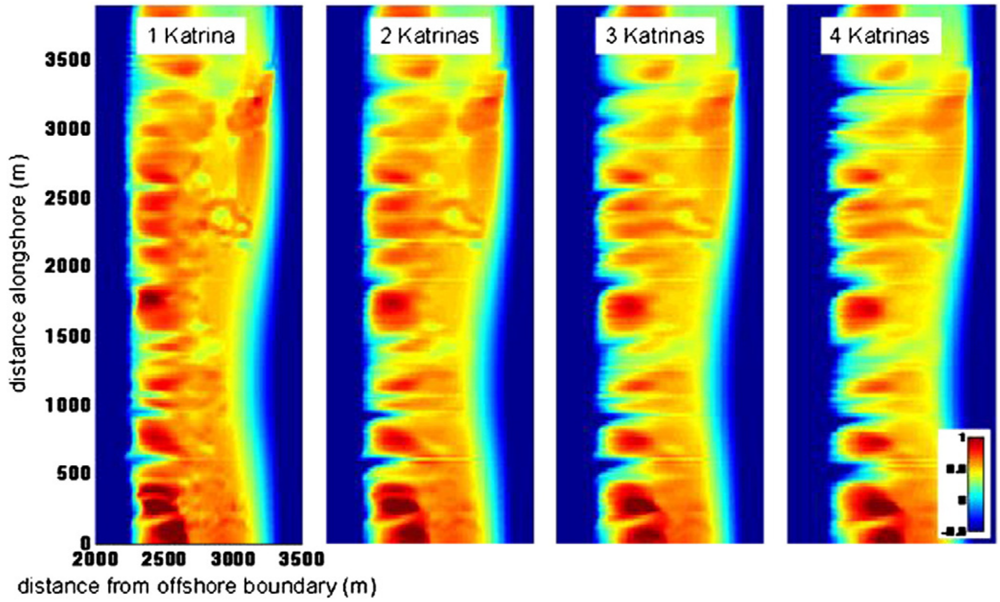

Fig. 9. Simulated island evolution after 1–4 consecutive storms. Color scale is elevation in meters.

where erosion occurred, would be predicted more accurately than the marsh and mud covered backbay area of the islands. XBeach correctly predicted erosion of the sandy berm (Fig. 6) and regions that were converted to open water. However, the locations that were subaerial both before and after the storm (Fig. 6) were not well-predicted. Sediment and other textural characteristics associated with the marsh substrate may explain these discrepancies.

5. Conclusions

It is important to be able to predict hurricane-induced barrier island erosion and accretion in order to evaluate the vulnerability of these coastlines. This study of the Chandeleur Islands, evaluated a coupled hydrodynamic and morphodynamic model, XBeach, in its ability to simulate tropical storms on low-lying barrier islands. The boundary conditions were obtained from pre-storm, lidar-derived bathymetry/topography. Model prediction skill was analyzed, and found to be robust. Model-predicted erosion patterns of the Chandeleur Islands were significantly correlated to observed erosion patterns ($R^2=0.4$). Subaerial island elevations decreased and the increase in island breaching and segmentation was well-predicted. Consistent with the observed response, the simulations did not produce an overwash fan.

The completion of a sensitivity study conducted using XBeach determined that subtle changes in the model configuration did not have substantial impacts on the simulation results, allowing the model user to have some freedom in choosing a resolution and morfacs that suits their study site. We did not find substantial sensitivity to plausible changes in the forcing (boundary) conditions. However, the model under predicted the observed erosion magnitude. While prediction errors could be due to fundamental inaccuracies of the model itself, we found that sensitivity to initial condition errors are due to the three year gap between the collection date of the lidar data and Hurricane Katrina's landfall. This was demonstrated by updating the initial conditions through successive morphologic simulations. Future low-lying barrier island case-studies using XBeach should focus on sites where detailed pre- and post-storm data are available from just before and just after the extreme event.

Acknowledgements

We would like to thank Kristy Guy (USGS) for drafting and image processing, Wayne Wright for lidar instrumentation development, and Charlene Sullivan (formerly with USGS) for lidar processing. Jim Flocks graciously provided his bathymetric data for construction of the morphology used to initialize the model. This work was funded by the University of Delaware and the U.S. Geological Survey's Coastal and Marine Geology Program.

References

Brock, J.C., Wright, C.W., Sallenger, A.H., Krabill, W.B., Swift, R.N., 2002. Basis and methods of NASA Airborne Topographic Mapper lidar surveys for coastal studies. Journal of Coastal Research 18 (1), 1–13.
Cañizares, R., Irish, J.L., 2008. Simulation of storm-induced barrier-island morphodynamics and flooding. Coastal Engineering 55, 1089–1101.
Cowell, P.J., Roy, P.S., Jones, R.A., 1995. Simulation of large-scale coastal change using a morphological-behaviour model. Marine Geology 126, 45–61.
Goldenberg, S.A., Landsea, C., Mestas-Nuñez, A., Gray, W., 2001. The recent increase in Atlantic hurricane activity: causes and implications. Science 293, 474–479.
Interagency Performance Evaluation Task Force, 2007. Performance Evaluation of the New Orleans and Southeast Louisiana Hurricane Protection System, Final Report of the Interagency Performance Evaluation Task Force, Vol. IV—the Storm. US Army Corps of Engineers, Washington, DC.
Jiménez, Sallenger, A.H., Fauver, L., 2006. Sediment Transport and Barrier Island Changes During Massive Overwash Events, 2006. ICCE, San Diego.
Kahn, J.H., 1986. Geomorphic recovery of the Chandeleur Islands, Louisiana, after a major hurricane. Journal of Coastal Research 2 (3), 337–344.
Knabb, R., Rhome, J., Brown, D., 2005. Tropical Cyclone Report: Hurricane Katrina. National Hurricane Center, Miami, FL.
Lesser, G., Roelvink, J.A., van Kester, J.A.T.M., Stelling, G.S., 2004. Development and validation of a three-dimensional morphological model. Coastal Engineering 51, 883–915.
Luettich Jr., R.A., Westerink, J.J., Scheffner, N.W., 1992. ADCIRC: an advanced three-dimensional circulation model for shelves, coasts and estuaries, report 1: theory and methodology of ADCIRC-2DDI and ADCIRC-3DL, Technical Report DRP-92-6. Department of the Army, US Army Corps of Engineers, Waterways Experiment Station, Vicksburg, MS, pp. 1–137.
McCall, R.T., Van Thiel de Vries, Plant, N.G., Van Dongeren, A.R., Roelvink, J.A., Thompson, D.M., Thompson, D.M., 2010. Two-dimensional time dependent Hurricane overwash and erosional modeling at Santa Rosa Island. Coastal Engineering 57 (7), 668–683.
Plant, N.G., Holland, K.T., Puleo, J.A., 2002. Analysis of the scale of errors in nearshore bathymetric data. Marine Geology 191, 71–86.
Plant, N.G., Edwards, K.L., Kaihatu, J.M., Veeramony, J., Hsu, L., Holland, K.T., 2009. The effect of bathymetric filtering on a nearshore process model. Coastal Engineering 56, 484–493.

Roelvink, J.A., Reniers, A., Van Dogeren, A., Van Thiel, J., de Vries, R., McCall, J. Lescinski, 2009. Modeling storm impacts on beaches, dunes and barrier islands. Coastal Engineering 56, 1133–1152.

Rosati, J.D., Stone, G.W., Dean, R.G., Kraus, N.C., 2006. Restoration of barrier islands overlying poorly-consolidated sediments, south-central Louisiana. Gulf Coast Association of Geological Societies Transactions 56, 727–740.

Sallenger Jr., A.H., 2000. Storm impact scale for barrier islands. Journal of Coastal Research 16 (3), 890–895.

Sallenger Jr., A.H., Wright, C.W., Howd, P., Doran, K., Guy, K., 2009. Chapter B. Extreme coastal changes on the Chandeleur Islands, Louisiana, during and after Hurricane Katrina. In: Lavoie, D. (Ed.), Sand Resources, Regional Geology, and Coastal Processes of the Chandeleur Islands Coastal System—an Evaluation of the Breton National Wildlife Refuge. U.S. Geological Survey Scientific Investigations Report 2009-5252, pp. 27–36.

Smith, J.M., Sherlock, A.R., Resio, D.T., 2001. STWAVE: Steady-State Spectral Wave Model User's Manual for STWAVE, Version 3.0. Coastal and Hydraulics Laboratory. U.S. Army Engineer Research and Development Center, Vicksburg, MS, pp. 1–81.

Stockdon, H., Sallenger, A., Holman, R., Howd, P., 2006. A simple model for the spatially-variable coastal response to hurricanes. Marine Geology 238, 1–20.

Stolper, D., List, J.H., Thieler, E.R., 2005. Simulating the evolution of coastal morphology and stratigraphy with a new morphological-behavior model (GEOMBEST). Marine Geology 218, 17–36.

Stone, G., Gyrmes, J., Dingler, J., Pepper, D., 1997. Overview and significance of hurricanes on the Louisiana coast, U.S.A. Journal of Coastal Research 13 (3), 656–669.

Twichell, D., Pendleton, E., Baldwin, W., Flocks, J., 2009. Subsurface control on seafloor erosional processes offshore of the Chandeleur Islands, Louisiana. Geo-Marine Letters 29, 349–358.

van Thiel de Vries, J.S.M., van Gent, M.R.A., Walstra, D.J.R., Reniers, A.J.H.M., 2008. Analysis of dune erosion in large scale flume experiments. Coastal Engineering 55 (12), 1028–1040.